Development of an Aptamer-Conjugated Polyrotaxane-Based Biodegradable Magnetic Resonance Contrast Agent for Tumor-Targeted Imaging

Zu, Guangyue; Cao, Yi; Dong, Jingjin; Zhou, Qihui; van Rijn, Patrick; Liu, Min; Pei, Renjun

Published in:
ACS Applied Bio Materials

DOI:
10.1021/acsabm.8b00639

Document Version
Publisher's PDF, also known as Version of record

Publication date:
2019

ACS APPLIED BIO MATERIALS
Cite This: ACS Appl. Bio Mater. 2019, 2, 406−416
Article
www.acsabm.org

Development of an Aptamer-Conjugated Polyrotaxane-Based Biodegradable Magnetic Resonance Contrast Agent for Tumor-Targeted Imaging

Guangyue Zu,[†,‡] Yi Cao,[†] Jingjin Dong,[∥] Qihui Zhou,[‡] Patrick van Rijn,[‡,∥] Min Liu,[*,§] and Renjun Pei[*,†]

[†]CAS Key Laboratory of Nano-Bio Interface, Division of Nanobiomedicine, Suzhou Institute of Nano-Tech and Nano-Bionics, Chinese Academy of Sciences, Suzhou 215123, China

[‡]Department of Biomedical Engineering, W. J. Kolff Institute for Biomedical Engineering and Materials Science, University of Groningen, University Medical Center Groningen, A. Deusinglaan 1, Groningen 9713 AV, The Netherlands

[§]Institute for Interdisciplinary Research, Jianghan University, Wuhan 430056, China

[∥]Zernike Institute for Advanced Materials, University of Groningen, Nijenborgh 4, Groningen 9747 AG, The Netherlands

Supporting Information

ABSTRACT: Gadolinium-based magnetic resonance imaging (MRI) contrast agents with biodegradability, biosafety, and high efficiency are highly desirable for tumor diagnosis. Herein, a biodegradable, AS1411-conjugated, α-cyclodextrin polyrotaxane-based MRI contrast agent (AS1411-G2(DTPA-Gd)-SS-PR) was developed for targeted imaging of cancer. The polyrotaxane-based contrast agent was achieved by the complexation of α-cyclodextrin (α-CD) and a linear poly(ethylene glycol) (PEG) chain containing disulfide linkages at two terminals. The disulfides enable the dethreading of the polyrotaxane into excretable small units due to cleavage of the disulfide linkages by reducing agents such as intracellular glutathione (GSH). Furthermore, the second-generation lysine dendron conjugated with gadolinium chelates and AS1411, a G-quadruplex oligonucleotide that has high binding affinity to nucleolin generally presenting a high level on the surface of tumor cells, coupled to the α-CD via click chemistry. The longitudinal relaxivity of AS1411-G2(DTPA-Gd)-SS-PR (11.7 mM^{-1} s^{-1}) was two times higher than the clinically used Gd-DTPA (4.16 mM^{-1} s^{-1}) at 0.5 T. The in vitro degradability was confirmed by incubating with 10 mM 1,4-dithiothreitol (DTT). Additionally, the cytotoxicity, histological assessment, and gadolinium retention studies showed that the prepared polyrotaxane-based contrast agent had a superior biocompatibility and was predominantly cleared renally without long-term accumulation toxicity. Importantly, AS1411-G2(DTPA-Gd)-SS-PR displayed the enhanced performance in MRI of breast cancer cells in vitro as well as a subcutaneous breast tumor in vivo due to the targeting ability of the AS1411 aptamer. The enhanced performance was due to efficient multivalent interactions with tumor cells, producing faster accumulation and longer contrast imaging time at the tumor site. This work clearly confirms that the specially designed and fabricated α-CD-based polyrotaxane is a promising contrast agent with an excellent contrast imaging performance and biosafety for tumor MR imaging.

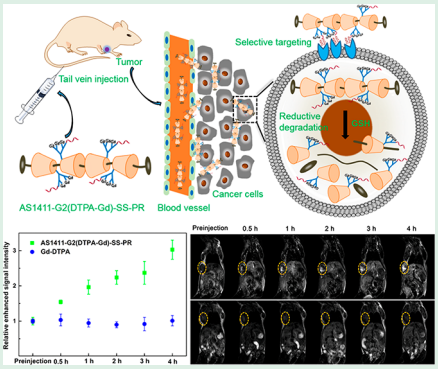

KEYWORDS: *polyrotaxanes, biodegradability, magnetic resonance imaging, AS1411 aptamer, breast cancer targeting*

INTRODUCTION

The delineation of the tumor boundary and the evaluation of tumor size are necessary for treatment planning and monitoring treatment response. Current guidelines incorporate the use of magnetic resonance imaging (MRI) because of its noninvasive nature, high spatiotemporal resolution, and lack of radiation.[1−3] However, most of the clinical magnetic resonance (MR) contrast agents are small molecular gadolinium (Gd) chelates, which have several inherent limitations due to their low molecular weight, like insufficient relaxivity and short circulation time.[4,5] As a result, the contrast-enhanced time window for MRI is very narrow, requiring repeated administration in high doses.[6,7] Macromolecule-based MRI contrast agents could potentially overcome those limitations due to their enhanced relaxivity derived from the prolonged rotational correlation time (τ_R), which is related to the large size of macromolecules.[8−11] Moreover, various functionalities are easily introduced into macromolecular contrast agents to further improve biocompatibility, circulation time in blood, accumulation in tumor site, and tumor target specificity.[12−15] A

Received: October 22, 2018
Accepted: December 24, 2018
Published: December 24, 2018

DOI: 10.1021/acsabm.8b00639
ACS Appl. Bio Mater. 2019, 2, 406−416

Scheme 1. Schematic Illustration of the Tumor-Targeting and the Reductive Biodegradability of the Biocleavable AS1411-Conjugated α-CD Polyrotaxane-Based MR Contrast Agent (AS1411-G2(DTPA-Gd)-SS-PR)

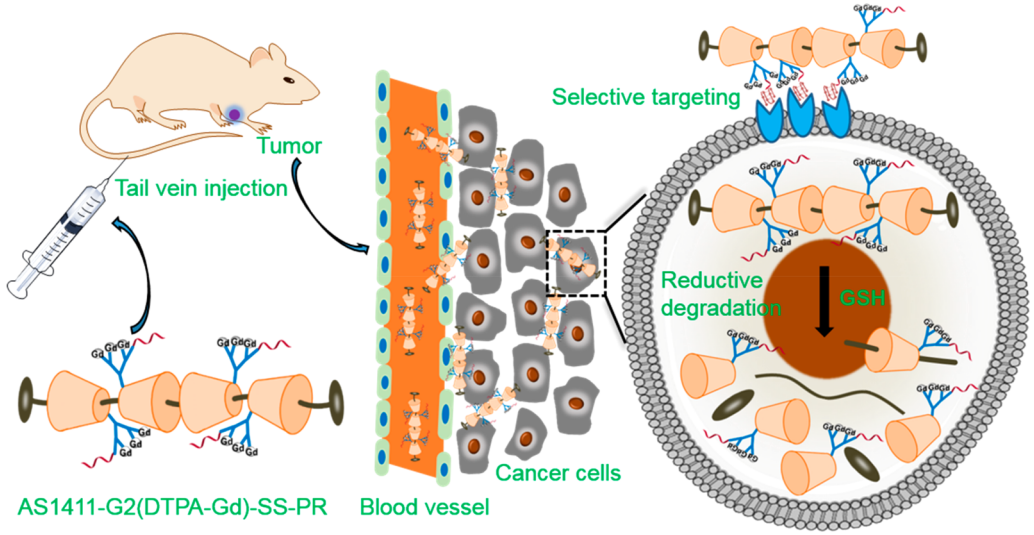

large number of macromolecular contrast agents have been developed by conjugating small molecular contrast agents to polymers,[16] dendrimers,[17,18] micelles,[19,20] proteins,[21,22] and supramolecular assemblies.[23−25]

Among the macromolecules used as MRI contrast agents, polyrotaxanes, a kind of noncovalently bound supramolecular material, are very promising because of their fascinating structural characteristics. First of all, the structure of polyrotaxanes is fabricated through threading cyclic molecules onto a polymer "axle" followed by capping with bulky end-caps to retain the threaded macrocycles.[26−28] Contrary to other macromolecules, polyrotaxanes are semirigid rod-like structures,[29] which could slow down the rotation of conjugated small molecular Gd chelates effectively increasing the relaxivity. Moreover, the rod-like structure of polyrotaxanes could effectively prolong the blood residence time increasing their chance of reaching target sites. Recent studies indicate that rod-like particles increase the circulation time in the blood due to lower macrophage internalization compared to globular macromolecules.[30,31] Additionally, accumulation at the tumor site is envisioned as rod-like structures able to move around obstacles and permeate into tumors through small leaky vasculatures, thereby efficiently making use of the enhanced permeation and retention effect (EPR), whereas globular macromolecules have to deform to pass through.[32] Besides, the semirigid rod-like structure of polyrotaxanes allows them to tumble and rotate easier via torque compared to globular structures, which increases the probability of close interactions with the wall of the tumor vessel and subsequently with tumor cells, further enhancing tumor accumulation.[33,34] Additionally, targeting ligand-conjugated polyrotaxane is advantageous because the ligand-bearing cyclic compounds are capable of spinning through the polymer chain as well as moving back and forth along the chain to maximize binding affinity between targeting ligands and receptors on the cell membrane to improve the retention effectiveness. This contrasts to the rigid spatial mismatch between the receptor and ligand of ligand-immobilized macromolecules.[35,36] On the basis of the above perspectives, polyrotaxanes are envisioned to be highly promising structures for designing and constructing MR contrast agents.

Another critical concern about designing Gd-based macromolecular contrast agents is biosafety. It is imperative to develop an MR contrast agent that not only has high contrast ability and long circulation time but also is readily eliminated from the body after performing diagnostic functions. Numerous research groups have designed a large variety of biodegradable macromolecular contrast agents based on in vivo microenvironment responses such as enzymes,[14,37] pH,[38,39] and redox reactions.[40] There are a few polyrotaxane-based MRI probes reported;[29,41] however, most of them cannot be excreted rapidly after MRI examination, leading to the potential accumulation of toxic Gd ions in tissues that may cause problems like nephrogenic systemic fibrosis.[42] It is therefore pertinent that the self-assembly threading structure of polyrotaxane is combined with designed dissociation and degradation to realize biodegradability.[43] Polymers containing disulfide bonds can rapidly degrade in the reductive intracellular cytoplasm.[44] Therefore, the disulfide linkage at both terminals of polyrotaxane used in this work was designed to be cleaved by the cellular redox environment, resulting in dethreading of polyrotaxane into easily excretable small units.

For specific targeting and retention at the tumor site, the 26-mer guanosine-rich oligonucleotide AS1411 was chosen as it has a strong binding affinity to nucleolin, a multifunctional protein overexpressed on the surface of a broad range of tumor cells, such as breast cancer and leukemia.[45−47] Researchers have used AS1411 as a targeting ligand to deliver therapeutic and imaging agents into the tumor region, and some studies have demonstrated that AS1411-conjugated materials can accumulate selectively in the tumor region.[48−50] AS1411 has several advantages compared to other targeting ligands such as antibodies including its smaller size and easier attachment allowing it to reach a higher density at the target site. In addition, AS1411 is stable against nuclease degradation in serum as a result of forming a G-quadruplex structure; furthermore, pharmacokinetic studies have shown an enhanced stability of AS1411 in blood in vivo.[45,51] More importantly, AS1411 is nonimmunogenic and has been proved to be safe in clinical trials.[52,53] Therefore, it is favorable to employ the AS1411 aptamer to construct tumor-targeted macromolecular MR contrast agents.

DOI: 10.1021/acsabm.8b00639
ACS Appl. Bio Mater. 2019, 2, 406−416

Herein, an AS1411-conjugated α-cyclodextrin (α-CD) polyrotaxane consisting of α-CD and poly(ethylene glycol) (PEG) capped with a bulky Z-tyrosine (Z-Tyr) and integrated with cytocleavable disulfide linkages was designed and fabricated to serve as a biodegradable tumor-targeted MRI contrast agent (AS1411-G2(DTPA-Gd)-SS-PR) (Scheme 1). Both α-CD and PEG have already been approved by the Food and Drug Administration (FDA) as drug formulations for human use, which would speed up the clinical translation of our developed probe. After capping, α-CD was modified with second-generation lysine dendron structures via click chemistry to carry high payloads of Gd chelates that further increases the relaxivity of a single macromolecule. Additionally, the use of cytocleavable disulfide linkages introduces biodegradability into the macromolecular MR contrast agent. To ensure selective accumulation in tumor tissue, AS1411 aptamers were conjugated to the surface of the prepared contrast agent by coupling with residual amino groups of lysine dendron. The chemical structure, relaxivity, biodegradability, and biocompatibility of AS1411-G2(DTPA-Gd)-SS-PR were characterized. Furthermore, in order to detect the targeting ability of AS1411-G2(DTPA-Gd)-SS-PR, the cellular MR imaging and in vivo MR imaging were performed using a human breast adenocarcinoma cell line (MCF-7 cells) and xenograft MCF-7 tumor-bearing mice.

EXPERIMENTAL SECTION

Materials. *N*,*N*′-Diisopropylethylamine (DIEA) and α-CD (99%) were acquired from J&K Co. Ltd. 1-(3-(Dimethylamino)propyl)-3-ethylcarbodiimide hydrochloride (EDC), *N*-hydroxysuccinimide (NHS), gadolinium chloride hexahydrate ($GdCl_3·6H_2O$), 1,4-dithiothreitol (DTT), and sodium ascorbate were purchased from Sigma-Aldrich. *N*-Benzyloxycarbonyl-L-tyrosine (Z-Tyr-OH) was purchased from Tokyo Chemical Industry Co. Ltd. 1-Hydroxybenzotrizole (HOBt, anhydrous) was obtained from GL Biochem Ltd. $CuSO_4·5H_2O$ (sp), ethylenediaminetetraacetic acid disodium salt (EDTA-2Na), and all the other chemicals of reagent grade were obtained from Sinopharm Chemical Reagent Co. Ltd. Propargyl carbonylimidazole (PA-CI) was prepared according to the previous literature.[54] The detailed synthesis process of α,ω-biscystamine PEG (PEG-SS-NH_2) and azido poly(L-lysine) dendron (N_3-lys-G2) are presented in the Supporting Information. ^{1}H NMR spectra were conducted to determine the chemical structure of PEG-SS-NH_2 (Figure S1) and N_3-lys-G2 (Figure S2). DNA oligos were synthesized and purified by Shanghai Sangon Biotechnology Co. Ltd. The DNA sequence is listed as follows.

5′HOOC6T-AS1411:

5′-COOH-T6-GGTGGTGGTGGTTGTGGTGGTGGTGG-3′

Synthesis of Z-Tyrosine-Terminated Cytocleavable Polyrotaxane (SS-PR). The procedure for the synthesis of cytocleavable SS-PR was performed according to previous literature with a slight modification.[55] PEG-SS-NH_2 (0.6 g, 0.14 mmol) was dissolved in 5 mL of Milli-Q water. Separately, a saturated α-CD solution was prepared by dissolving α-CD (10.8 g, 11.1 mmol) in 70 mL of Milli-Q water. The PEG-SS-NH_2 solution was added to the saturated α-CD solution, and the system was stirred for 24 h at room temperature (rt), during which a white precipitate of pseudopolyrotaxane (SS-PPR) was obtained. After centrifugation at 7000 rpm for 1 h, the supernatant was removed, and the precipitate was freeze-dried for 1 day to obtain SS-PPR (5.62 g, 83.5% yield) as a white powder. ^{1}H NMR (400 MHz, DMSO-d_6): δ 3.25−3.41 (m, C(4)***H*** and C(2)***H*** of α-CD), 3.50 (br, CH_2CH_2O of PEG), 3.54−3.79 (C(6)***H***, C(3)***H*** and C(5)***H*** of α-CD), 4.48 (m, C(6)O***H*** of α-CD), 4.80 (m, C(1)***H*** of α-CD), 5.43−5.53 (m, C(2, 3)O***H*** of α-CD).

For the capping reaction of pseudopolyrotaxane, the end-cap reagent Z-Tyr-OH (2.05 g, 6.5 mmol), coupling reagents HOBt (0.88 g, 6.5 mmol), benzotriazol-1-yloxy-tris(dimethylamino)-phosphonium hexafluorophosphate (BOP) (2.88 g, 6.5 mmol), and DIEA (1.13 mL, 6.5 mmol) were dissolved in 4 mL of dried dimethylformamide (DMF), and the mixture was added to SS-PPR (5.62 g). The resulting reaction mixture was stirred for 24 h (rt). After the reaction, the solution was poured into methanol to precipitate the polyrotaxane, which was then collected by centrifugation and washed twice with acetone and Milli-Q water to remove unreacted end-cap reagent and coupling reagents. The obtained precipitation was redissolved in dimethyl sulfoxide (DMSO), which then was poured into water to precipitate the polyrotaxane and washed three times with 50 °C Milli-Q water to remove unreacted α-CD and PEG. Finally, the recovered product, Z-Tyr-terminated SS-PR, was obtained by drying in a vacuum at 60 °C for 72 h (3.12 g, 0.115 mmol, 81.7% yield). ^{1}H NMR (400 MHz, DMSO-d_6): δ 3.50 (s, CH_2CH_2O of PEG), 3.23−3.74 (m, C(4)***H***, C(2)***H***, C(6)***H***, C(3)***H*** and C(5)***H*** of α-CD), 4.44 (m, C(6)O***H*** of α-CD), 4.79 (m, C(1)***H*** of α-CD), 5.47−5.67 (m, C(2, 3)O***H*** of α-CD), 6.63 (d, ***H*** of Tyr), 7.03 (d, ***H*** of Tyr), 7.30 (m, ***H*** of Cbz group).

Synthesis of Alkynyl-Modified Cytocleavable Polyrotaxane (alk-SS-PR). SS-PR (1.0 g, 0.0367 mmol, 15.2 mmol available OH-groups) was dissolved in 15 mL of dried DMSO. PA-CI (2.28 g, 15.2 mmol) in 10 mL of dried DMSO was added to the solution of SS-PR and stirred for 48 h at 50 °C under a nitrogen atmosphere. After the reaction, this solution was poured into diethyl ether to precipitate the alkynyl polyrotaxane, which was then collected by filtration. This purification process was repeated three times to remove the unreacted reagents, and the final precipitation was collected, washed with diethyl ether, and dried in a vacuum at 50 °C to obtain alk-SS-PR (0.8 g, 35.6% yield). ^{1}H NMR (400 MHz, DMSO-d_6): δ 2.55 (s, CHCCH_2O), 3.50 (s, CH_2CH_2O of PEG), 3.23−3.74 (m, C(4)***H***, C(2)***H***, C(6)***H***, C(3)***H*** and C(5)***H*** of α-CD), 4.2 (C(2)***H*** of α-CD), 4.60−4.80 (C(6)O***H***, C(1)***H*** of α-CD), 5.18 (CHCCH_2O), 6.64 (d, ***H*** of Tyr), 7.07 (d, ***H*** of Tyr), 7.31 (m, ***H*** of Cbz group).

Synthesis of Second-Generation Lysine Dendron-Grafted Cytocleavable Polyrotaxane (G2-SS-PR). The coupling of the azido second-generation poly(L-lysine) dendron (N_3-lys-G2) to the alkynyl-modified cytocleavable polyrotaxane (alk-SS-PR) was conducted by the click reaction. Briefly, alk-SS-PR (0.79 g) and N_3-lys-G2 (1.61 g, 3.33 mmol) were dissolved in 80 mL of DMSO in a Schlenk tube and purged with nitrogen to remove the oxygen. $CuSO_4·5H_2O$ (26.4 mg, 0.106 mmol) and sodium ascorbate (65.6 mg, 0.331 mmol), both dissolved in 1 mL of deoxygenated water, were sequentially added into the solution via a syringe. The mixture was stirred under a nitrogen atmosphere at 50 °C for 48 h. After removing most of the solvent by vacuum distillation, the remaining concentrate was dissolved in 15 mL of Milli-Q water and dialyzed against water using a dialysis tube (MWCO = 3500 Da) and freeze-dried to obtain G2-SS-PR (1.03 g, 64.6% yield). ^{1}H NMR (400 MHz, D_2O): δ 1.28−2.01 (m, CHCH_2CH_2CH_2CH_2), 3.04 (m, C$H_2$$NH_2$), 3.26 (m, C$H_2$NH), 3.45 (s, C$H_2CH_2$O of PEG), 3.73 (s, triazole ring-CH_2NH), 3.78−4.65 (m, ***H*** of α-CD, CON***H***), 5.36 (m, CON***H***), 8.17 (s, ***H*** of triazole ring).

Synthesis of DTPA-Gd-Modified Cytocleavable Polyrotaxane (G2(DTPA-Gd)-SS-PR). First, diethylenetriaminepentacetate acid (DTPA) was conjugated onto G2-SS-PR through EDC-mediated coupling. Briefly, G2-SS-PR (0.9 g) and DTPA (5.9 g, 15.0 mmol) were dissolved in 30 mL of Milli-Q water, and the pH of the solution was adjusted to pH 6 with *N*,*N*,*N*′,*N*′-tetramethylethylenediamine (TMEDA) followed by the addition of EDC (1.15 g, 6.0 mmol) to the solution and stirring (rt). After 6 h, the product was purified by dialysis using a dialysis tube (MWCO = 3500 Da) and freeze-dried to obtain G2(DTPA)-SS-PR (1.01 g). ^{1}H NMR (400 MHz, D_2O): δ 1.24−2.23 (m, CHCH_2CH_2CH_2CH_2), 3.03 (m, C$H_2$$NH_2$), 3.28 (m, C$H_2$NH), 3.46 (s, C$H_2CH_2$O of PEG), 3.65, 3.88, 3.92 (s, CH_2 of DTPA), 3.73 (s, triazole ring-CH_2), 3.61−4.65 (***H*** of α-CD, CON***H***), 5.36 (m, CON***H***), 8.14 (s, ***H*** of triazole ring).

DOI: 10.1021/acsabm.8b00639
ACS Appl. Bio Mater. 2019, 2, 406−416

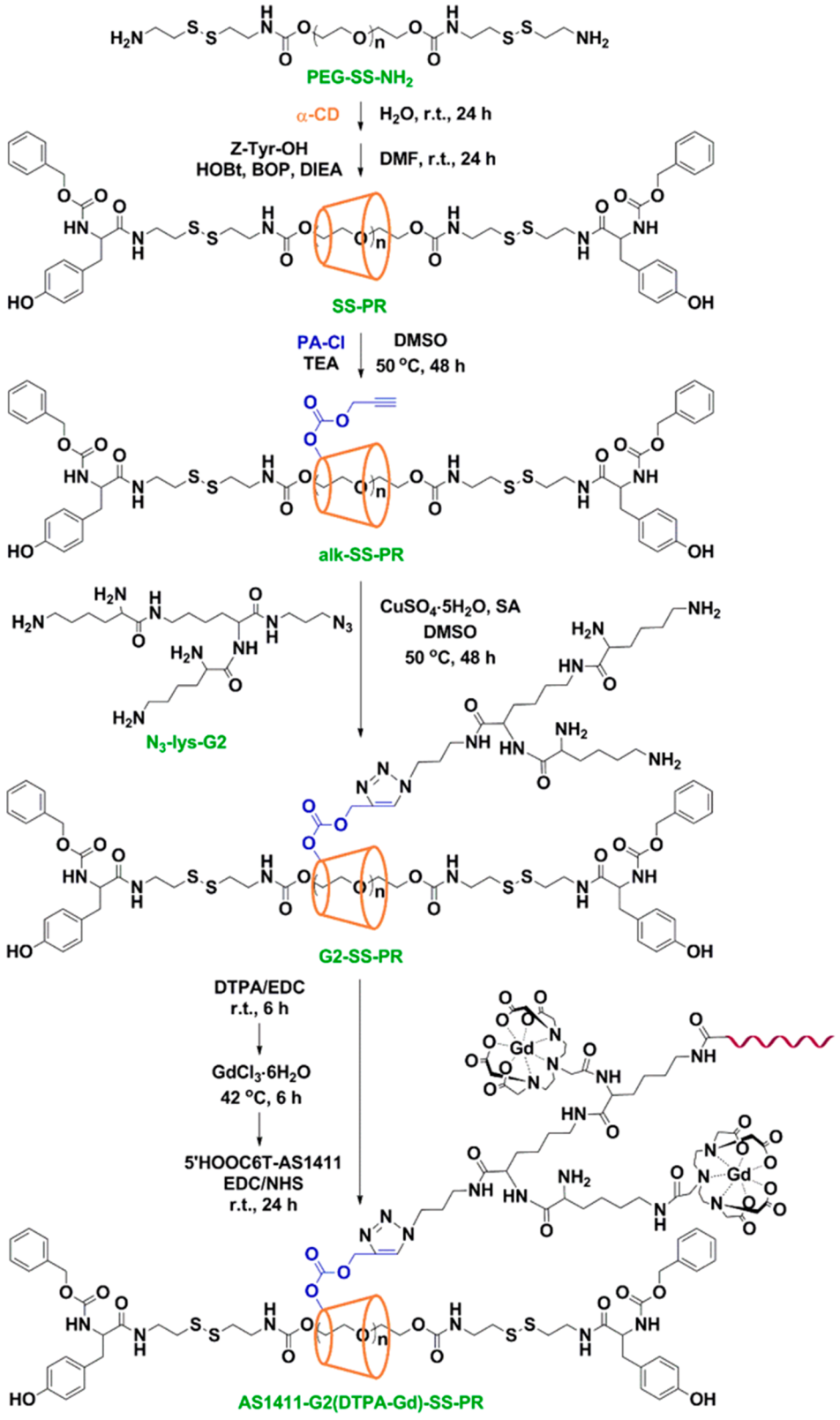

Figure 1. Synthetic schematic route of the biocleavable AS1411-conjugated α-CD polyrotaxane-based MR contrast agent.

To chelate with Gd^{3+}, G2(DTPA)-SS-PR (0.9 g) was dissolved in 30 mL of 0.1 M citrate buffer (pH = 5.6). $GdCl_3 \cdot 6H_2O$ (0.51 g, 1.37 mmol) was dissolved in 5 mL of Milli-Q water and was added to the solution of G2(DTPA)-SS-PR. The pH of the solution was maintained at 6 with 1 M NaOH. Afterward, the mixture was stirred at 42 °C for 6 h. The unreacted Gd^{3+} was removed by dialysis against 10 mM EDTA-2Na solution and water using a dialysis tube (MWCO = 3500 Da). Afterward, the product G2(DTPA-Gd)-SS-PR (0.54 g) was obtained through freeze-drying.

Synthesis of AS1411-Labeled G2(DTPA-Gd)-SS-PR (AS1411-G2(DTPA-Gd)-SS-PR). 5′HOOC6T-AS1411 was conjugated to G2-(DTPA-Gd)-SS-PR through the residual amino groups of lysine

DOI: 10.1021/acsabm.8b00639
ACS Appl. Bio Mater. 2019, 2, 406−416

dendron by EDC/NHS coupling reaction. Briefly, 5′HOOC6T-AS1411 (32 μL, 1.92 μmol) and EDC (37 μL, 10 mg/mL) were mixed in 100 μL of PBS (10 mM, pH 7.4) and stirred at 37 °C for 15 min for the activation of COOH. Afterward, NHS (22.1 μL, 10 mg/mL) and G2(DTPA-Gd)-SS-PR (100 μL, 500 mg/mL) were added to the above solution. The mixture was stirred at 37 °C for 24 h, and the unreacted 5′HOOC6T-AS1411 was removed by centrifugal filter devices (MWCO = 30000 Da). The final product AS1411-G2(DTPA-Gd)-SS-PR was then obtained by freeze-drying. The conjugation of 5′HOOC6T-AS1411 was detected by UV−vis absorption spectra.

Longitudinal Relaxivity and MRI of Solution. For the measurement of the longitudinal relaxation time (T_1), the AS1411-G2(DTPA-Gd)-SS-PR solutions of different Gd concentrations (0.25, 0.5, 1, 1.5, 2, 2.5 mM) were prepared. Gd-DTPA at the same concentration series was used as a control. For the measurement of T_1-weighted MR images, the AS1411-G2(DTPA-Gd)-SS-PR solutions of different Gd concentrations (0.125, 0.25, 0.5, 1, 2 mM) were prepared. Gd-DTPA at the same concentration series was used as a control. The detailed procedures are shown in the Supporting Information.

In Vitro Degradation of AS1411-G2(DTPA-Gd)-SS-PR. Longitudinal relaxivity of the biocleavable AS1411-G2(DTPA-Gd)-SS-PR in the presence of DTT was conducted. The AS1411-G2(DTPA-Gd)-SS-PR solutions of different Gd concentrations (0.031, 0.063, 0.125, 0.25, 0.5, 1 mM) were prepared and incubated with DTT (10 mM) in PBS buffer at 37 °C. Then T_1 of the solution was measured at 0, 0.5, 1, 2, 4, 24, 48, 72, 96, 120, 144, and 168 h. The T_1 measurement method and r_1 calculation method were the same as those in the Longitudinal Relaxivity and MRI of Solution section.

In Vitro MRI Study. The cellular MRI study was conducted by a 1.5 T small animal magnetic resonance imager. MCF-7 cells, over-expressing nucleolin on the surface,[56] were treated with AS1411-G2(DTPA-Gd)-SS-PR, G2(DTPA-Gd)-SS-PR, and Gd-DTPA for 2 h, and the Gd amount was 0.2 mmol. The procedures followed the previous work,[57] and the details are shown in the Supporting Information.

In Vivo MR Imaging. The subcutaneous breast cancer animal model was introduced to female athymic nude mice. Following the procedures of previous work,[57] the tumor-bearing mice were injected with AS1411-G2(DTPA-Gd)-SS-PR, G2(DTPA-Gd)-SS-PR, and Gd-DTPA. The T_1-weighted images were acquired by a 1.5 T small animal magnetic resonance imager, and the detailed procedures are shown in the Supporting Information. All animal experiments were carried out under the guide of the relevant laws and institutional guidelines.

Biocompatibility Study. The cytotoxicity of AS1411-G2(DTPA-Gd)-SS-PR against human umbilical vein endothelial cells (HUVEC) was evaluated by a water-soluble tetrazolium salts (WST) assay. Gd-DTPA was selected as a control. Additionally, the hematoxylin and eosin (H&E) staining was employed to evaluate the in vivo tissue toxicity of AS1411-G2(DTPA-Gd)-SS-PR. In vivo gadolinium retention was employed and evaluated after intravenous injection of AS1411-G2(DTPA-Gd)-SS-PR. The detailed experimental procedures are shown in the Supporting Information.

Statistical Analysis. The OriginPro 9.0 program was used for statistical analysis, and the results were presented as mean ± standard deviation (SD). $*p < 0.05$, $**p < 0.01$, and $***p < 0.001$ were considered statistically significant.

RESULTS AND DISCUSSION

Synthesis and Characterization of AS1411-G2(DTPA-Gd)-SS-PR. To achieve a high sensitivity and specificity for tumor-targeted MRI, and ensure the biosafety for in vivo applications, we developed an AS1411-conjugated biocleavable polyrotaxane as a tumor-targeted MRI contrast agent. The polyrotaxane composed of a reductively cleavable terminated PEG axle and α-CD rotor capped with Z-Tyr was synthesized as a scaffold. To covalently graft the azido second-generation poly(L-lysine) dendron on the surface of α-CD with a high selectivity and yield under mild conditions, the Cu^I-catalyzed click chemistry has been used, followed by conjugation of the Gd chelates. Finally, the AS1411 was conjugated to the surface of the MRI contrast agent by coupling with a residual amino group of the lysine dendron. The detailed synthetic process of AS1411-G2(DTPA-Gd)-SS-PR is shown in Figure 1.

The Z-Tyr-terminated cleavable polyrotaxane was prepared by a two-phase process. First, the prepared axle PEG-SS-NH_2 was added to the saturated aqueous solution of α-CD. α-CD spontaneously formed inclusion complexes with PEG through host−guest recognition. A substantial amount of white precipitate appeared after 30 min, which is the pseudopolyrotaxane SS-PPR. The chemical structure of SS-PPR was verified using the ^{1}H NMR spectrum and is shown in Figure S3. Then the SS-PPR was dissolved in anhydrous DMF, and the bulky Z-Tyr-OH end-caps were bound to the PEG chain-ends by the coupling agent BOP and HOBt to confine the α-CD to the PEG axle. In order to minimize dethreading of the α-CD from the PEG axle, pseudopolyrotaxane was dissolved in concentrated solution during the addition of the end-caps Z-Tyr-OH. The number of CDs threaded onto the PEG axle was calculated to be 23 by comparing the value for the integral area of the ^{1}H NMR signal between 4.79 ppm (C(1) proton of α-CD) and 3.23−3.74 ppm (CH_2CH_2O of the PEG axle and C(2), C(3), C(4), C(5), and C(6) protons of α-CD), which is shown in Figure S3. Compared with the ^{1}H NMR spectrum of SS-PPR, the ^{1}H NMR spectrum of SS-PR shows a characteristic Z-tyrosine signal at 6.63−7.30 ppm, indicating that the capping reaction has occurred. In addition, the signal of PEG is separated from those of α-CD in the ^{1}H NMR spectrum of SS-PPR, which indicates that SS-PPR is in the dethreading state in DMSO-d_6 before capping, while the signals of PEG and α-CD overlap after capping. This shift indicates that there is interaction between PEG and α-CD after capping, affecting the distribution of the characteristic signals on the spectrum. Furthermore, the threading of α-CD onto PEG was demonstrated using XRD analysis. As shown in Figure S4, both of the patterns of SS-PPR and SS-PR have main sharp reflections $2\theta = 20°$, representing the channel-type structure of polyrotaxane consistent with α-CD and PEG.

Afterward, surface functionalization with alkynyl was performed using PA-CI that reacted with the α-CD hydroxy groups. The ^{1}H NMR spectrum of alk-SS-PR is shown in Figure S3, and the signal of alkynyl appeared at 2.55 ppm, which proves the successful modification with alkynyl. The modification with alkynyl was also confirmed by FT-IR as shown in Figure S5 by the characteristic signal of alkynyl appearing at 2129 cm^{-1} when comparing the FT-IR spectrum of SS-PR, and after surface functionalization with alkynyl. Then, the N_3-lys-G2 was covalently coupled to the surface of polyrotaxane using the click reaction with an alkyne group to obtain the lysine dendron-grafted cytocleavable polyrotaxane (G2-SS-PR). The ^{1}H NMR spectrum is shown in Figure S6. Compared with the spectrum of alk-SS-PR, the new signals at 1.28−2.01, 3.04, and 3.26 ppm are the characteristic signal of methylene of N_3-lys-G2 and the characteristic signal at 8.17 ppm proved the forming of the triazole ring during the click reaction. Furthermore, the alkyne IR signal at 2129 cm^{-1} is significantly reduced as shown in Figure S5.

Finally, DTPA was covalently bound to the amino group of N_3-lys-G2 by EDC chemistry. The ^{1}H NMR spectrum of G2(DTPA)-SS-PR is shown in Figure S6, with new signals at 3.65, 3.88, and 3.92 ppm attributed to the characteristic signals

DOI: 10.1021/acsabm.8b00639
ACS Appl. Bio Mater. 2019, 2, 406−416

for the methylene group of DTPA, indicating that the surface of polyrotaxane has been successfully modified with DTPA. Thereafter, the targeting molecule AS1411 was coupled to the residual amino groups on the surface of G2(DTPA-Gd)-SS-PR with the carboxyl group of 5′HOOC6T-AS1411 using EDC/NHS coupling conditions. The UV−vis absorbance of AS1411-G2(DTPA-Gd)-SS-PR at 260 nm demonstrates that 5′HOOC6T-AS1411 was successfully conjugated onto G2-(DTPA-Gd)-SS-PR as shown in Figure S7.

Relaxivity Properties. Relaxivity is a key indicator to identify the imaging performance of MR contrast agents. To evaluate the relaxivity properties of the prepared AS1411-G2(DTPA-Gd)-SS-PR, the longitudinal relaxation time and T_1-weighted image of aqueous solution at different Gd concentrations were measured, with Gd-DTPA evaluated as a control group. As shown in Figure 2a, after linear fitting, the

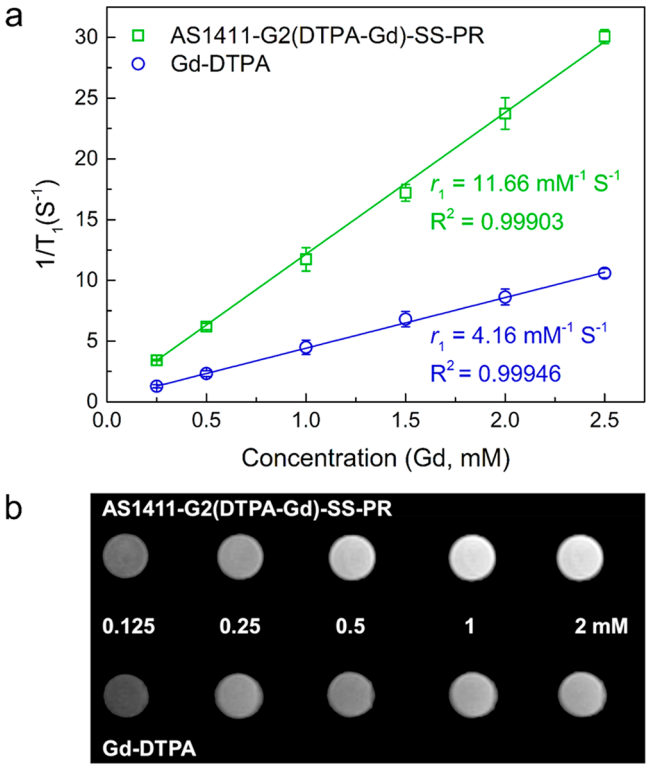

Figure 2. (a) T_1 relaxation rate $(1/T_1)$ with a series of Gd concentrations for AS1411-G2(DTPA-Gd)-SS-PR and Gd-DTPA in aqueous solution. (b) T_1-weighted MR images of aqueous solution with a series of Gd concentrations of AS1411-G2(DTPA-Gd)-SS-PR and Gd-DTPA.

longitudinal relaxivity r_1 of AS1411-G2(DTPA-Gd)-SS-PR is 11.7 mM^{-1} s^{-1}, which is nearly 2 times higher than Gd-DTPA (4.16 mM^{-1} s^{-1}). The T_1-weighted images of both AS1411-G2(DTPA-Gd)-SS-PR and Gd-DTPA exhibit an improved brightness with an increasing Gd concentration. However, at the same Gd concentration, the images of the AS1411-G2(DTPA-Gd)-SS-PR are significantly brighter than that of Gd-DTPA as shown in Figure 2b. These results indicate that the polyrotaxane-based contrast agent AS1411-G2(DTPA-Gd)-SS-PR has an enhanced contrast performance compared to the clinical small-molecule contrast agent Gd-DTPA. According to Bloembergen−Solomon−Morgan theory,[58] the main factor that contributes to the improved longitudinal relaxivity is the increased τ_R of Gd chelate. The conjugation to the large polyrotaxane effectively slows down the molecular rotation causing τ_R to increase. Additionally, the semirigid structure of polyrotaxane prevents Gd chelates from being shielded from water, as would be the case for conventional coiling flexible macromolecular contrast agents, thereby guaranteeing sufficient accessibility to water protons. Furthermore, the dense conjugation of Gd chelates to the polyrotaxane increases the local concentrations of Gd. The results demonstrate that the developed AS1411-G2(DTPA-Gd)-SS-PR is a promising MR contrast agent.

In Vitro Degradation. To obtain a biodegradable MR contrast agent, we introduced the disulfide linkage at both terminals of the polyrotaxane. Reducing agents should cleave the disulfide linkage and initiate slow dethreading of the polyrotaxane into excretable products. To evaluate the biodegradability of AS1411-G2(DTPA-Gd)-SS-PR, MRI contrast agents with various Gd concentrations were incubated in PBS solution with 10 mM DTT at 37 °C to mimic the reducing environment in vivo. The change of relaxivity with incubation time was determined by measuring the longitudinal relaxation time T_1 to calculate r_1 (shown in Figure 3). During

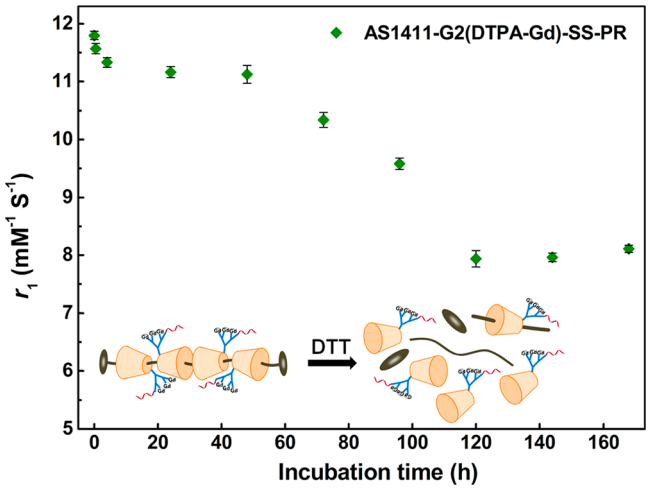

Figure 3. Variation of longitudinal relaxivity r_1 of AS1411-G2(DTPA-Gd)-SS-PR treated with 10 mM DTT over time.

the first hour of incubation, r_1 quickly decreases from 11.8 mM^{-1} s^{-1} to 11.3 mM^{-1} s^{-1}. As r_1 is proportional to the size, the decrease of r_1 indicates that α-CD bonding with Gd chelates starts slowly dethreading from the PEG axle, which demonstrates that the disulfide linkage was cleaved by DTT. Afterward, r_1 decreases to 8.0 mM^{-1} s^{-1} and remains constant at a value of 8.1 mM^{-1} s^{-1}. The further decrease of r_1 comes from the further dethreading of α-CD; at the end, the equilibrium between threading and dethreading completely shifted, and as a result, the r_1 remains around 8.1 mM^{-1} s^{-1}, which is comparable with the reported free α-CD-Gd.[41] This result indicates that the prepared cleavable polyrotaxane-based contrast agent is likely to be biodegradable via disulfide cleavage due to the presence of reducing agents.

In Vitro MR Imaging of Breast Cancer Cells. To evaluate the targeting specificity of AS1411-G2(DTPA-Gd)-SS-PR, the in vitro MRI study on MCF-7 cells was performed. The MCF-7 cells overexpress nucleolin, to which the AS1411 binds. As control groups, the cells treated with nontargeting G2(DTPA-Gd)-SS-PR and Gd-DTPA were chosen and

DOI: 10.1021/acsabm.8b00639
ACS Appl. Bio Mater. 2019, 2, 406−416

untreated cells were used as blank group. The T_1-weighted cellular MR images are shown in Figure 4a. Compared to the

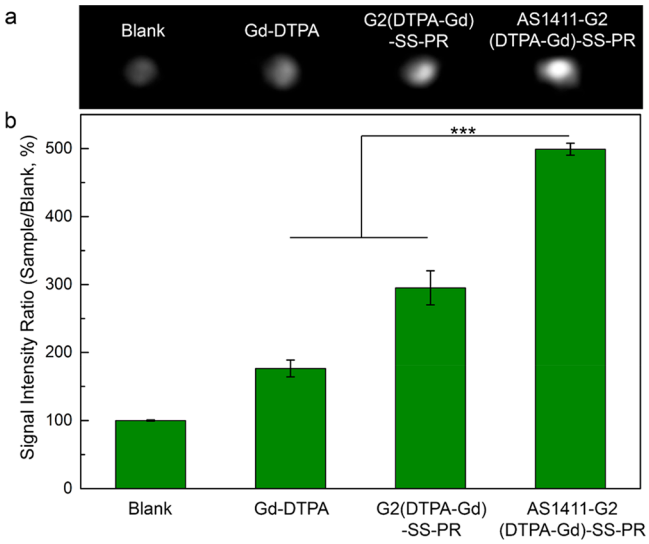

Figure 4. (a) Cellular MR images of MCF-7 cells treated with Gd-DTPA, G2(DTPA-Gd)-SS-PR, and AS1411-G2(DTPA-Gd)-SS-PR at 0.2 mM Gd concentration for 2 h, respectively. Untreated cells were used as the blank group. (b) Signal intensity ratio of cellular MR images for all groups. Signal intensity shows a statistically significant difference (***$p < 0.001$, $n = 4$).

untreated cells, images of all groups incubated with contrast agents are brighter. The G2(DTPA-Gd)-SS-PR-treated group exhibits a slightly brighter image than the Gd-DTPA-treated group. However, the group incubated with AS1411-G2-(DTPA-Gd)-SS-PR exhibits the brightest image. This was confirmed by quantitative analysis by determining the signal intensity values using ImageJ software. The signal intensity of the untreated group is set at 100%, and the results are shown in Figure 4b. The signal intensity ratios of Gd-DTPA, G2(DTPA-Gd)-SS-PR, and AS1411-G2(DTPA-Gd)-SS-PR-treated group to the blank are 176 ± 12%, 295 ± 25%, and 499 ± 9%, respectively. The signal intensity ratio for AS1411-G2(DTPA-Gd)-SS-PR bearing the targeting ligand is about 1.7-fold higher than that of the nontargeting G2(DTPA-Gd)-SS-PR group. All of these results indicate that AS1411-G2(DTPA-Gd)-SS-PR is able to target the breast cancer cells and that the target ability, specifically, is due to the strong binding affinity between the AS1411 aptamer and nucleolin.

In Vivo MRI Study of Tumor-Bearing Mice. For further application on tumor diagnosis, the MRI was conducted using MCF-7 tumor-bearing mice to examine whether AS1411-G2(DTPA-Gd)-SS-PR could help to effectively improve the sensitivity and accuracy of in vivo tumor imaging for nucleolin-overexpressed tumors, indicative for human breast cancer. Tumor-bearing mice were randomly divided into three groups and intravenously injected with Gd-DTPA, G2(DTPA-Gd)-SS-PR, and AS1411-G2(DTPA-Gd)-SS-PR with a 0.1 mmol/kg Gd dose, respectively. The T_1-weighted coronal MR images were acquired preinjection and various time points after injection. As shown in Figure 5a, within the acquired time points, there is no enhanced contrast between the tumor and surrounding tissue of the group injected with Gd-DTPA. As for the group injected with the nontargeting contrast agent G2(DTPA-Gd)-SS-PR, from the time point of 0.5 h after

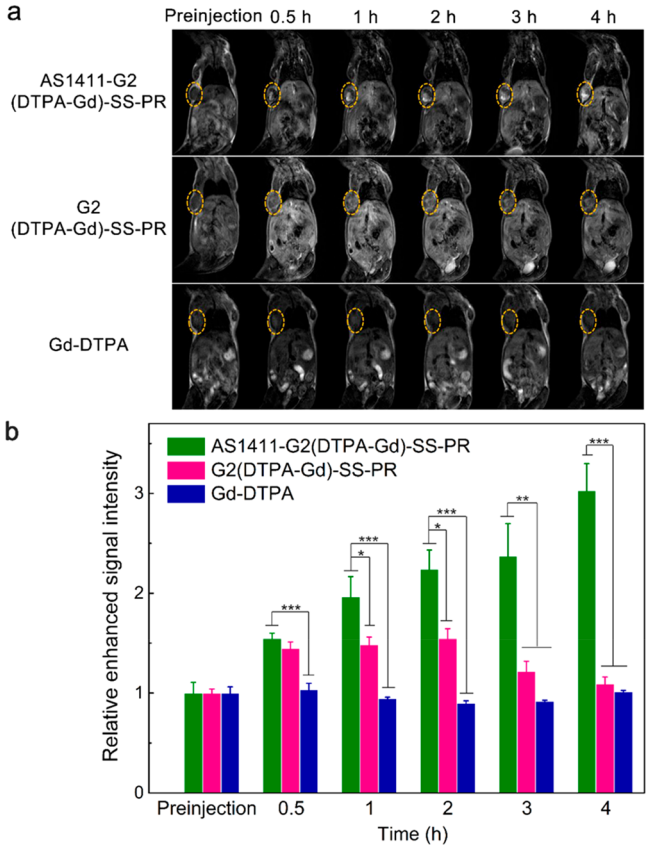

Figure 5. (a) The T_1-weighted coronal images of the MCF-7 tumor-bearing mice injected with AS1411-G2(DTPA-Gd)-SS-PR, G2-(DTPA-Gd)-SS-PR, and Gd-DTPA at preinjection and after injection for 0.5, 1, 2, 3, and 4 h. The yellow dotted circle shows the tumor location. (b) RESI of the tumor region in the groups of AS1411-G2(DTPA-Gd)-SS-PR, G2(DTPA-Gd)-SS-PR, and Gd-DTPA. The RESI was calculated by the signal intensity of postinjection dividing preinjection. RESI shows a statistically significant difference (*$p < 0.05$, **$p < 0.01$, ***$p < 0.001$, $n = 5$).

administration, there is a modest increase in MR signal in the tumor region and a slight further enhancement in the following 1.5 h, with a subsequent gradual decrease in brightness. However, for the AS1411-G2(DTPA-Gd)-SS-PR group, an obvious contrast enhancement of the tumor region compared to the surrounding tissue is observed at 0.5 h after injection, and further enhanced over time in both brightness and contrast. Additionally, the tumor showed clear boundaries when AS1411-G2(DTPA-Gd)-SS-PR was used.

To better show the contrast enhancement of the tumor site by contrast agents, a quantification analysis of the signal intensity at the tumor site is necessary. We set the signal intensity before injection as 1.0, and the relative enhanced signal intensity (RESI) after injection was calculated with ImageJ software. As shown in Figure 5b, there is negligible RESI at the tumor region when Gd-DTPA was used at all of the time points, which is understandable since Gd-DTPA suffered a rapid clearance from the circulation because of the small molecular weight. In contrast, the group injected with G2(DTPA-Gd)-SS-PR presents an increased RESI of 1.4 of the tumor region at 2 h after injection, but decreases slowly to 1.1 at 4 h after injection. However, the RESI of tumor region contrasted by AS1411-G2(DTPA-Gd)-SS-PR rapidly reaches 1.5 at 0.5 h after injection, and increases substantially over

DOI: 10.1021/acsabm.8b00639
ACS Appl. Bio Mater. 2019, 2, 406−416

time, displaying a 3 times enhancement at 4 h after injection. These results indicate that both G2(DTPA-Gd)-SS-PR and AS1411-G2(DTPA-Gd)-SS-PR can produce apparent contrast between the tumor region and normal tissue. However, the RESI of the tumor region contrast by AS1411-G2(DTPA-Gd)-SS-PR is higher than that of G2(DTPA-Gd)-SS-PR at each time point. Additionally, the AS1411-G2(DTPA-Gd)-SS-PR contrast agent keeps increasing the RESI at least until 4 h after injection. The better performance of AS1411-G2(DTPA-Gd)-SS-PR compared to G2(DTPA-Gd)-SS-PR with respect to a faster accumulation and longer residence time can be attributed to the targeting specificity of AS1411 aptamer.

Since the image acquisition parameters and injection dose of contrast agents of each group are the same, the contrast enhancement generated by AS1411-G2(DTPA-Gd)-SS-PR is mainly attributed to the special structure and target molecule of the contrast agent. The semirigid rod-like structure of polyrotaxane increases the rotation-related time of the Gd complex, and the high load of Gd provided by the second-generation lysine dendron greatly increases the relaxation efficiency. Moreover, as mentioned before, the semirigid rod-like structure of AS1411-G2(DTPA-Gd)-SS-PR provides a longer blood circulation time, which is beneficial for tumor region accumulation and thus remains for enough time for MRI. In addition, the special molecular structure of polyrotaxane makes the recognition of the modified targeting molecule a great advantage. The α-CD on the PEG axle is free to rotate and slide within a certain range, which allows the modified AS1411 aptamer to have a greater opportunity to bind to nucleolin on the cell surface to achieve multivalent targeting. Hence, both the efficient targeting ability of AS1411 and the multivalent approach help AS1411-G2(DTPA-Gd)-SS-PR accumulate faster and retain contrast for a longer time at the tumor site. The above factors offer the polyrotaxane-based contrast agent AS1411-G2(DTPA-Gd)-SS-PR with an excellent contrast imaging performance, namely, provide a high sensitivity, tumor specificity, and long imaging time for tumor MRI.

Cytotoxicity. The cytotoxicity of AS1411-G2(DTPA-Gd)-SS-PR is the primary consideration prior to their in vitro and in vivo imaging applications. The cytotoxicity of AS1411-G2(DTPA-Gd)-SS-PR to HUVEC cells was conducted by a WST cell proliferation assay to evaluate its biocompatibility. Gd-DTPA was used as a control. As shown in Figure 6, the cell viability of AS1411-G2(DTPA-Gd)-SS-PR is about 100% even when the concentration of Gd is raised to 5.00 mM, which is comparable to Gd-DTPA. The results indicate that the prepared polyrotaxane-based contrast agent has negligible toxicity to normal cells, confirming that AS1411-G2(DTPA-Gd)-SS-PR has a good cytocompatibility at high Gd concentrations.

Histological Assessment. H&E staining was used to test the in vivo tissue toxicity of AS1411-G2(DTPA-Gd)-SS-PR. As shown in Figure 7, compared with the control group not receiving any contrast agent, there are no appreciable morphological changes nor obvious damage found in the main organs of the groups injected with AS1411-G2(DTPA-Gd)-SS-PR, even at a higher Gd dose. Typically, there are no signs of inflammatory or necrosis from hepatocytes and no pulmonary fibrosis in lung sections. In general, all of the investigated organs appeared normal, and the histopathological changes are negligible, suggesting the AS1411-G2(DTPA-Gd)-SS-PR contrast agent does not produce any in vivo toxicity to the mice in 2 days.

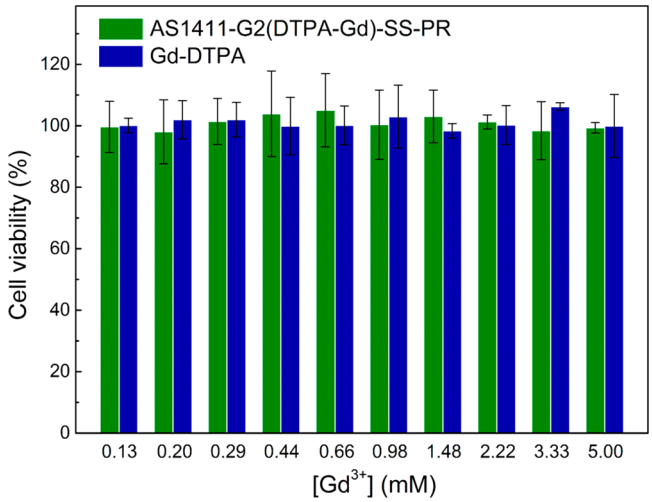

Figure 6. Cell viability of AS1411-G2(DTPA-Gd)-SS-PR and Gd-DTPA with various Gd concentrations in HUVEC cells after incubation for 24 h.

Retention Study. Generally, molecular species and nanomaterials may enter different organs via blood circulation after intravenous injection. For Gd-based contrast agents, one of the drawbacks is systematic toxicity, because the accumulated contrast agents are able to be internalized by healthy cells and metabolized into toxic Gd^{3+}.[42] To investigate the metabolic activity and long-term toxicity of the prepared polyrotaxane-based contrast agent, in vivo retention study of Gd in liver, spleen, kidney, lung, heart, and muscle was quantified in healthy mice. As shown in Figure 8, the residual amounts of Gd in the liver, spleen, kidney, lung, heart, and muscle are 0.038%, 0.057%, 0.49%, 0.0069%, 0.014%, and 0.0062% per tissue or organ, respectively. The result suggests that Gd is mostly accumulated in the kidney after 10 days, indicating that AS1411-G2(DTPA-Gd)-SS-PR mainly passes through the kidney metabolism, which could be attributed to the biodegradability of the cleavable polyrotaxane-based contrast agents containing disulfide bonds. In addition, the Gd retention in other main tissues and organs is on the same order of magnitude with the small molecular contrast agent Gd-(DTPA-BMA) as reported but significantly lower than the reported macromolecular contrast agent PAMAM-G6-(GdDO3A) (liver >5%, muscle >3%, spleen >1%, kidney >1%).[59,60] The data demonstrate that the cleavable polyrotaxane-based contrast agent has a few long-term residues in major organs and tissues. Taken together, we demonstrate that the prepared AS1411-G2(DTPA-Gd)-SS-PR is biocompatible to mice and can be metabolized by the mice, which is crucial for biomedical applications.

CONCLUSIONS

To summarize, we prepared a semirigid, rod-like, AS1411-conjugated, biocleavable α-CD-based polyrotaxane (AS1411-G2(DTPA-Gd)-SS-PR) as a biodegradable tumor-targeting MR contrast agent. The polyrotaxane-based contrast agent was produced by threading α-CD onto a PEG "axle" followed by capping with bulky Z-Tyr end-caps through cytocleavable disulfide linkages. Then the α-CD was modified with a second-generation lysine dendron to upload the imaging element, Gd

DOI: 10.1021/acsabm.8b00639
ACS Appl. Bio Mater. 2019, 2, 406−416

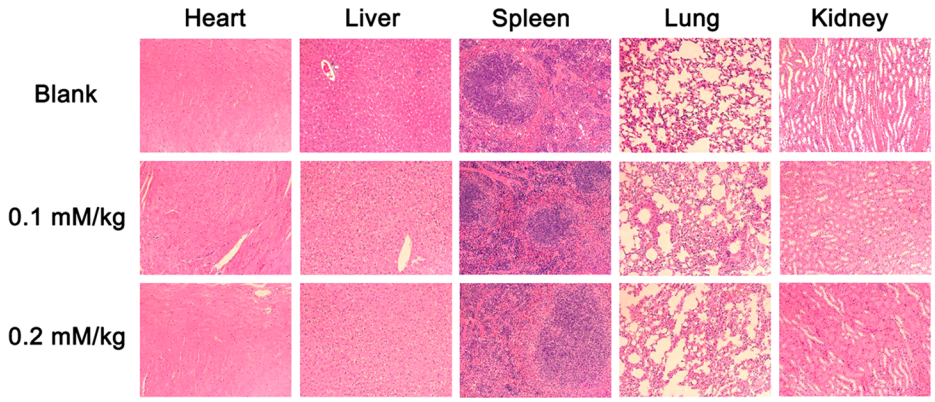

Figure 7. H&E-stained section images (200× magnification) of major organs of mice treated with AS1411-G2(DTPA-Gd)-SS-PR for 2 days at the Gd dose of 0.1 mmol/kg and 0.2 mmol/kg. The mice treated with physiological saline were used as a blank group.

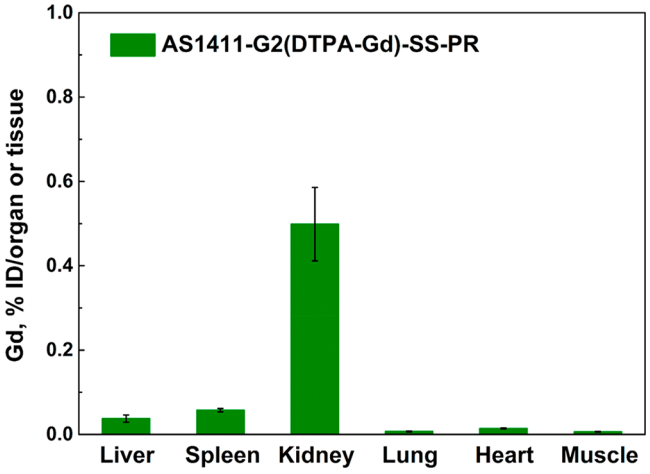

Figure 8. Retention of the Gd ion in main organs and tissues of mice (n = 5), including liver, spleen, kidney, lung, heart, and muscle, at 10 days after injection of AS1411-G2(DTPA-Gd)-SS-PR.

chelates, and target molecule, AS1411, on the surface. The longitudinal relaxivity of AS1411-G2(DTPA-Gd)-SS-PR is 11.7 mM^{-1} s^{-1} ,which is nearly 2 times higher than the commercial Gd-DTPA. Moreover, the in vitro degradation study indicated that α-CD with conjugated Gd chelates slowly dethread from the PEG chain upon cleavage of the terminal disulfide bonds. The results indicated that the prepared contrast agent had a good biocompatibility and did not accumulate in the major organs but rather was cleared via the kidneys and did not display long-term accumulation toxicity both in vitro and in vivo. Furthermore, due to the efficient targeting ability of AS1411 aptamer, AS1411-G2(DTPA-Gd)-SS-PR outperforms the conventional Gd-DTPA by having a faster accumulation at the tumor site along with a longer contrast imaging time. Therefore, AS1411-G2(DTPA-Gd)-SS-PR is a promising macromolecular contrast agent with an excellent contrast imaging performance and biosafety for tumor MRI.

■ ASSOCIATED CONTENT

Supporting Information

The Supporting Information is available free of charge on the ACS Publications website at DOI: 10.1021/acsabm.8b00639.

Materials and instruments; detailed synthesis procedures and characterization of N_3-lys-G2 and PEG-SS-NH_2; ^1H NMR spectra, FT-IR absorption spectra, X-ray diffraction pattern, and UV−vis spectra; detailed procedures of longitudinal relaxivity and MRI of solution, in vitro MRI study, cell culture, animal subcutaneous tumor model, in vivo MR imaging, cytotoxicity assay, histological assessment of mice, and analysis of gadolinium accumulation in mice experiments (PDF)

■ AUTHOR INFORMATION

Corresponding Authors

*E-mail: mliu2010@sinano.ac.cn.
*E-mail: rjpei2011@sinano.ac.cn. Tel: 86-512-62872776.

ORCID

Yi Cao: 0000-0001-7590-2373
Qihui Zhou: 0000-0003-2474-4197
Patrick van Rijn: 0000-0002-2208-5725
Min Liu: 0000-0003-4779-8489
Renjun Pei: 0000-0002-9353-3935

Notes

The authors declare no competing financial interest.

■ ACKNOWLEDGMENTS

This work was financially supported by the National Natural Science Foundation of China (21775160, 21807107, and 81801837), the National Key Research and Development program (2016YFA0101500), the Science and Technology Foundation of Jiangsu Province (BE2018665, BK20161262, BK20180251, BK20180256, and BK20180258), and the CAS/SAFEA International Innovation Teams program. G.Z. and Q.Z. are very grateful for financial support from the China Scholarship Council (201706890012 and 201406630003). The authors thank Dr. Brandon Peterson for proofreading the manuscript.

■ REFERENCES

(1) Alonzi, R.; Hoskin, P. Functional Imaging in Clinical Oncology: Magnetic Resonance Imaging- and Computerised Tomography-Based Techniques. *Clin. Oncol.* **2006**, *18*, 555−570.
(2) Carin, A. J.; Moliere, S.; Gabriele, V.; Lodi, M.; Thiebaut, N.; Neuberger, K.; Mathelin, C. Relevance of Breast MRI in Determining the Size and Focality of Invasive Breast Cancer Treated by Mastectomy: a Prospective Study. *World J. Surg. Oncol.* **2017**, *15*, 8.
(3) Shi, X. Y.; Wang, S. H.; Swanson, S. D.; Ge, S.; Cao, Z. Y.; Van Antwerp, M. E.; Landmark, K. J.; Baker, J. R. Dendrimer-Functionalized Shell-Crosslinked Iron Oxide Nanoparticles for In-

DOI: 10.1021/acsabm.8b00639
ACS Appl. Bio Mater. 2019, 2, 406−416

Vivo Magnetic Resonance Imaging of Tumors. *Adv. Mater.* **2008**, *20*, 1671−1678.
(4) Geraldes, C.; Laurent, S. Classification and Basic Properties of Contrast Agents for Magnetic Resonance Imaging. *Contrast Media Mol. Imaging* **2009**, *4*, 1−23.
(5) Mi, P.; Kokuryo, D.; Cabral, H.; Wu, H. L.; Terada, Y.; Saga, T.; Aoki, I.; Nishiyama, N.; Kataoka, K. A pH-Activatable Nanoparticle with Signal-Amplification Capabilities for Non-Invasive Imaging of Tumour Malignancy. *Nat. Nanotechnol.* **2016**, *11*, 724−730.
(6) Tang, J. B.; Sheng, Y. Q.; Hu, H. J.; Shen, Y. Q. Macromolecular MRI Contrast Agents: Structures, Properties and Applications. *Prog. Polym. Sci.* **2013**, *38*, 462−502.
(7) Venditto, V. J.; Regino, C. A. S.; Brechbiel, M. W. PAMAM Dendrimer Based Macromolecules as Improved Contrast Agents. *Mol. Pharmaceutics* **2005**, *2* (4), 302−311.
(8) Botta, M.; Tei, L. Relaxivity Enhancement in Macromolecular and Nanosized GdIII-Based MRI Contrast Agents. *Eur. J. Inorg. Chem.* **2012**, *2012*, 1945−1960.
(9) Li, Y.; Beija, M.; Laurent, S.; vander Elst, L.; Muller, R. N.; Duong, H. T. T.; Lowe, A. B.; Davis, T. P.; Boyer, C. Macromolecular Ligands for Gadolinium MRI Contrast Agents. *Macromolecules* **2012**, *45*, 4196−4204.
(10) Huang, R. Q.; Han, L.; Li, J. F.; Liu, S. H.; Shao, K.; Kuang, Y. Y.; Hu, X.; Wang, X. X.; Lei, H.; Jiang, C. Chlorotoxin-Modified Macromolecular Contrast Agent for MRI Tumor Diagnosis. *Biomaterials* **2011**, *32*, 5177−5186.
(11) Luo, K.; Liu, G.; He, B.; Wu, Y.; Gong, Q. Y.; Song, B.; Ai, H.; Gu, Z. W. Multifunctional Gadolinium-Based Dendritic Macromolecules as Liver Targeting Imaging Probes. *Biomaterials* **2011**, *32*, 2575−2585.
(12) Ye, M. Z.; Qian, Y.; Tang, J. B.; Hu, H. J.; Sui, M. H.; Shen, Y. Q. Targeted Biodegradable Dendritic MRI Contrast Agent for Enhanced Tumor Imaging. *J. Controlled Release* **2013**, *169*, 239−245.
(13) Esser, L.; Truong, N. P.; Karagoz, B.; Moffat, B. A.; Boyer, C.; Quinn, J. F.; Whittaker, M. R.; Davis, T. P. Gadolinium-Functionalized Nanoparticles for Application as Magnetic Resonance Imaging Contrast Agents via Polymerization-Induced Self-Assembly. *Polym. Chem.* **2016**, *7*, 7325−7337.
(14) Guo, C. H.; Sun, L.; Cai, H.; Duan, Z. Y.; Zhang, S. Y.; Gong, Q. Y.; Luo, K.; Gu, Z. W. Gadolinium-Labeled Biodegradable Dendron-Hyaluronic Acid Hybrid and Its Subsequent Application as a Safe and Efficient Magnetic Resonance Imaging Contrast Agent. *ACS Appl. Mater. Interfaces* **2017**, *9*, 23508−23519.
(15) Zhang, Y.; Zou, T. J.; Guan, M. R.; Zhen, M. M.; Chen, D. Q.; Guan, X. P.; Han, H. B.; Wang, C. R.; Shu, C. Y. Synergistic Effect of Human Serum Albumin and Fullerene on Gd-DO3A for Tumor-Targeting Imaging. *ACS Appl. Mater. Interfaces* **2016**, *8*, 11246−11254.
(16) Cao, Y.; Liu, M.; Zhang, K. C.; Dong, J. J.; Zu, G. Y.; Chen, Y.; Zhang, T. T.; Xiong, D. S.; Pei, R. J. Preparation of Linear Poly(glycerol) as a T-1 Contrast Agent for Tumor-Targeted Magnetic Resonance Imaging. *J. Mater. Chem. B* **2016**, *4*, 6716−6725.
(17) Sena, L. M.; Fishman, S. J.; Jenkins, K. J.; Xu, H.; Brechbiel, M. W.; Regino, C. A. S.; Kosaka, N.; Bernardo, M.; Choyke, P. L.; Kobayashi, H. Magnetic Resonance Lymphangiography with a Nano-Sized Gadolinium-Labeled Dendrimer in Small and Large Animal Models. *Nanomedicine* **2010**, *5*, 1183−1191.
(18) Zu, G. Y.; Tong, X. Y.; Zhang, T. T.; Cao, Y.; Kuang, Y.; Zhang, K. C.; Zhang, Y. J.; Luo, L. Q.; Liu, M.; Pei, R. J. PEGylated Chitosan Grafted with Polyamidoamine-Dendron as Tumor-Targeted Magnetic Resonance Imaging Contrast Agent. *New J. Chem.* **2017**, *41*, 7689−7696.
(19) Cao, Y.; Liu, M.; Zhang, K. C.; Zu, G. Y.; Kuang, Y.; Tong, X. Y.; Xiong, D. S.; Pei, R. J. Poly(glycerol) Used for Constructing Mixed Polymeric Micelles as T-1 MRI Contrast Agent for Tumor-Targeted Imaging. *Biomacromolecules* **2017**, *18*, 150−158.
(20) Cao, Y.; Liu, M.; Kuang, Y.; Zu, G. Y.; Xiong, D. S.; Pei, R. J. A Poly(epsilon-caprolactone)-Poly(glycerol)-Poly(epsilon-caprolactone) Triblock Copolymer for Designing a Polymeric Micelle as a Tumor Targeted Magnetic Resonance Imaging Contrast Agent. *J. Mater. Chem. B* **2017**, *5*, 8408−8416.
(21) Karfeld-Sulzer, L. S.; Waters, E. A.; Davis, N. E.; Meade, T. J.; Barron, A. E. Multivalent Protein Polymer MRI Contrast Agents: Controlling Relaxivity via Modulation of Amino Acid Sequence. *Biomacromolecules* **2010**, *11*, 1429−1436.
(22) Karfeld-Sulzer, L. S.; Waters, E. A.; Kohlmeir, E. K.; Kissler, H.; Zhang, X. M.; Kaufman, D. B.; Barron, A. E.; Meade, T. J. Protein Polymer MRI Contrast Agents: Longitudinal Analysis of Biomaterials In Vivo. *Magn. Reson. Med.* **2011**, *65*, 220−228.
(23) Martinelli, J.; Thangavel, K.; Tei, L.; Botta, M. Dendrimeric beta-Cyclodextrin/Gd-III Chelate Supramolecular Host-Guest Adducts as High-Relaxivity MRI Probes. *Chem. - Eur. J.* **2014**, *20*, 10944−10952.
(24) Battistini, E.; Gianolio, E.; Gref, R.; Couvreur, P.; Fuzerova, S.; Othman, M.; Aime, S.; Badet, B.; Durand, P. High-Relaxivity Magnetic Resonance Imaging (MRI) Contrast Agent Based on Supramolecular Assembly between a Gadolinium Chelate, a Modified Dextran, and Poly-beta-Cyclodextrin. *Chem. - Eur. J.* **2008**, *14*, 4551−4561.
(25) Sun, M.; Zhang, H. Y.; Liu, B. W.; Liu, Y. Construction of a Supramolecular Polymer by Bridged Bis(permethyl-beta-cyclodextrin)s with Porphyrins and Its Highly Efficient Magnetic Resonance Imaging. *Macromolecules* **2013**, *46*, 4268−4275.
(26) Harada, A.; Hashidzume, A.; Yamaguchi, H.; Takashima, Y. Polymeric Rotaxanes. *Chem. Rev.* **2009**, *109*, 5974−6023.
(27) Harada, A.; Takashima, Y.; Yamaguchi, H. Cyclodextrin-Based Supramolecular Polymers. *Chem. Soc. Rev.* **2009**, *38*, 875−882.
(28) Li, J.; Loh, X. J. Cyclodextrin-Based Supramolecular Architectures: Syntheses, Structures, and Applications for Drug and Gene Delivery. *Adv. Drug Delivery Rev.* **2008**, *60*, 1000−1017.
(29) Zhou, Z. X.; Mondjinou, Y.; Hyun, S. H.; Kulkarni, A.; Lu, Z. R.; Thompson, D. H. Gd^{3+}-1,4,7,10-Tetraazacyclododecane-1,4,7-triacetic-2-hydroxypropyl-beta-cyclodextrin/Pluronic Polyrotaxane as a Long Circulating High Relaxivity MRI Contrast Agent. *ACS Appl. Mater. Interfaces* **2015**, *7*, 22272−22276.
(30) Geng, Y.; Dalhaimer, P.; Cai, S. S.; Tsai, R.; Tewari, M.; Minko, T.; Discher, D. E. Shape Effects of Filaments Versus Spherical Particles in Flow and Drug Delivery. *Nat. Nanotechnol.* **2007**, *2*, 249−255.
(31) Sharma, G.; Valenta, D. T.; Altman, Y.; Harvey, S.; Xie, H.; Mitragotri, S.; Smith, J. W. Polymer Particle Shape Independently Influences Binding and Internalization by Macrophages. *J. Controlled Release* **2010**, *147*, 408−412.
(32) Truong, N. P.; Whittaker, M. R.; Mak, C. W.; Davis, T. P. The Importance of Nanoparticle Shape in Cancer Drug Delivery. *Expert Opin. Drug Delivery* **2015**, *12*, 129−142.
(33) Gentile, F.; Chiappini, C.; Fine, D.; Bhavane, R. C.; Peluccio, M. S.; Cheng, M. M. C.; Liu, X.; Ferrari, M.; Decuzzi, P. The Effect of Shape on the Margination Dynamics of Non-Neutrally Buoyant Particles in Two-Dimensional Shear Flows. *J. Biomech.* **2008**, *41*, 2312−2318.
(34) Toy, R.; Peiris, P. M.; Ghaghada, K. B.; Karathanasis, E. Shaping Cancer Nanomedicine: the Effect of Particle Shape on the In Vivo Journey of Nanoparticles. *Nanomedicine* **2014**, *9*, 121−134.
(35) Cairo, C. W.; Gestwicki, J. E.; Kanai, M.; Kiessling, L. L. Control of Multivalent Interactions by Binding Epitope Density. *J. Am. Chem. Soc.* **2002**, *124*, 1615−1619.
(36) Ooya, T.; Yui, N. Multivalent Interactions between Biotin-Polyrotaxane Conjugates and Streptavidin as a Model of New Targeting for Transporters. *J. Controlled Release* **2002**, *80*, 219−228.
(37) Cai, H.; Wang, X. J.; Zhang, H.; Sun, L.; Pan, D. Y.; Gong, Q. Y.; Gu, Z. W.; Luo, K. Enzyme-Sensitive Biodegradable and Multifunctional Polymeric Conjugate as Theranostic Nanomedicine. *Applied Materials Today* **2018**, *11*, 207−218.
(38) Wei, X. L.; Luo, Q.; Sun, L.; Li, X.; Zhu, H. Y.; Guan, P. J.; Wu, M.; Luo, K.; Gong, Q. Y. Enzyme- and pH-Sensitive Branched Polymer-Doxorubicin Conjugate-Based Nanoscale Drug Delivery

DOI: 10.1021/acsabm.8b00639
ACS Appl. Bio Mater. 2019, 2, 406−416

System for Cancer Therapy. *ACS Appl. Mater. Interfaces* **2016**, *8*, 11765−11778.
(39) Schopf, E.; Sankaranarayanan, J.; Chan, M. N.; Mattrey, R.; Almutairi, A. An Extracellular MRI Polymeric Contrast Agent That Degrades at Physiological pH. *Mol. Pharmaceutics* **2012**, *9*, 1911−1918.
(40) Luo, Q.; Xiao, X. Y.; Dai, X. H.; Duan, Z. Y.; Pan, D.; Zhu, H. Y.; Li, X.; Sun, L.; Luo, K.; Gong, Q. Y. Cross-Linked and Biodegradable Polymeric System as a Safe Magnetic Resonance Imaging Contrast Agent. *ACS Appl. Mater. Interfaces* **2018**, *10*, 1575−1588.
(41) Fredy, J. W.; Scelle, J.; Guenet, A.; Morel, E.; Adam de Beaumais, S.; Menand, M.; Marvaud, V.; Bonnet, C. S.; Toth, E.; Sollogoub, M.; Vives, G.; Hasenknopf, B. Cyclodextrin Polyrotaxanes as a Highly Modular Platform for the Development of Imaging Agents. *Chem. - Eur. J.* **2014**, *20*, 10915−10920.
(42) Aime, S.; Caravan, P. Biodistribution of Gadolinium-Based Contrast Agents, Including Gadolinium Deposition. *J. Magn. Reson. Imaging* **2009**, *30*, 1259−1267.
(43) Inada, T.; Tamura, A.; Terauchi, M.; Yamaguchi, S.; Yui, N. A Silencing-Mediated Enhancement of Osteogenic Differentiation by Supramolecular Ternary siRNA Polyplexes Comprising Biocleavable Cationic Polyrotaxanes and Anionic Fusogenic Peptides. *Biomater. Sci.* **2018**, *6*, 440−450.
(44) Son, S.; Namgung, R.; Kim, J.; Singha, K.; Kim, W. J. Bioreducible Polymers for Gene Silencing and Delivery. *Acc. Chem. Res.* **2012**, *45*, 1100−1112.
(45) Bates, P. J.; Reyes-Reyes, E. M.; Malik, M. T.; Murphy, E. M.; O'Toole, M. G.; Trent, J. O. G-Quadruplex Oligonucleotide AS1411 as a Cancer-Targeting Agent: Uses and Mechanisms. *Biochim. Biophys. Acta, Gen. Subj.* **2017**, *1861*, 1414−1428.
(46) Malik, M. T.; O'Toole, M. G.; Casson, L. K.; Thomas, S. D.; Bardi, G. T.; Reyes-Reyes, E. M.; Ng, C. K.; Kang, K. A.; Bates, P. J. AS1411-Conjugated Gold Nanospheres and Their Potential for Breast Cancer Therapy. *Oncotarget* **2015**, *6*, 22270−22281.
(47) Soundararajan, S.; Wang, L.; Sridharan, V.; Chen, W. W.; Courtenay-Luck, N.; Jones, D.; Spicer, E. K.; Fernandes, D. J. Plasma Membrane Nucleolin Is a Receptor for the Anticancer Aptamer AS1411 in MV4−11 Leukemia Cells. *Mol. Pharmacol.* **2009**, *76*, 984−991.
(48) Deng, R.; Shen, N.; Yang, Y.; Yu, H. L.; Xu, S. P.; Yang, Y. W.; Liu, S. J.; Meguellati, K.; Yan, F. Targeting Epigenetic Pathway with Gold Nanoparticles for Acute Myeloid Leukemia Therapy. *Biomaterials* **2018**, *167*, 80−90.
(49) Taghdisi, S. M.; Danesh, N. M.; Ramezani, M.; Yazdian-Robati, R.; Abnous, K. A Novel AS1411 Aptamer-Based Three-Way Junction Pocket DNA Nanostructure Loaded with Doxorubicin for Targeting Cancer Cells In Vitro and In Vivo. *Mol. Pharmaceutics* **2018**, *15*, 1972−1978.
(50) Mosafer, J.; Abnous, K.; Tafaghodi, M.; Mokhtarzadeh, A.; Ramezani, M. In Vitro and In Vivo Evaluation of Anti-Nucleolin-Targeted Magnetic PLGA Nanoparticles Loaded with Doxorubicin as a Theranostic Agent for Enhanced Targeted Cancer Imaging and Therapy. *Eur. J. Pharm. Biopharm.* **2017**, *113*, 60−74.
(51) Liu, J.; Wei, T.; Zhao, J.; Huang, Y. Y.; Deng, H.; Kumar, A.; Wang, C. X.; Liang, Z. C.; Ma, X. W.; Liang, X. J. Multifunctional Aptamer-Based Nanoparticles for Targeted Drug Delivery to Circumvent Cancer Resistance. *Biomaterials* **2016**, *91*, 44−56.
(52) Bates, P. J.; Laber, D. A.; Miller, D. M.; Thomas, S. D.; Trent, J. O. Discovery and Development of the G-Rich Oligonucleotide AS1411 as a Novel Treatment for Cancer. *Exp. Mol. Pathol.* **2009**, *86*, 151−164.
(53) Rosenberg, J. E.; Bambury, R. M.; Van Allen, E. M.; Drabkin, H. A.; Lara, P. N.; Harzstark, A. L.; Wagle, N.; Figlin, R. A.; Smith, G. W.; Garraway, L. A.; Choueiri, T.; Erlandsson, F.; Laber, D. A. A Phase II Trial of AS1411 (a Novel Nucleolin-Targeted DNA Aptamer) in Metastatic Renal Cell Carcinoma. *Invest. New Drugs* **2014**, *32*, 178−187.
(54) De Geest, B. G.; Van Camp, W.; Du Prez, F. E.; De Smedt, S. C.; Demeester, J.; Hennink, W. E. Biodegradable Microcapsules Designed via 'Click' Chemistry. *Chem. Commun.* **2008**, 190−192.
(55) Yamashita, A.; Yui, N.; Ooya, T.; Kano, A.; Maruyama, A.; Akita, H.; Kogure, K.; Harashima, H. Synthesis of a Biocleavable Polyrotaxane-Plasmid DNA (pDNA) Polyplex and Its Use for the Rapid Nonviral Delivery of pDNA to Cell Nuclei. *Nat. Protoc.* **2007**, *1*, 2861−2869.
(56) Soundararajan, S.; Chen, W. W.; Spicer, E. K.; Courtenay-Luck, N.; Fernandes, D. J. The Nucleolin Targeting Aptamer AS1411 Destabilizes Bcl-2 Messenger RNA in Human Breast Cancer Cells. *Cancer Res.* **2008**, *68*, 2358−2365.
(57) Zu, G. Y.; Kuang, Y.; Dong, J. J.; Cao, Y.; Wang, K. W.; Liu, M.; Luo, L. Q.; Pei, R. J. Multi-Arm Star-Branched Polymer as An Efficient Contrast Agent for Tumor-Targeted Magnetic Resonance Imaging. *J. Mater. Chem. B* **2017**, *5*, 5001−5008.
(58) Caravan, P.; Ellison, J. J.; McMurry, T. J.; Lauffer, R. B. Gadolinium(III) Chelates as MRI Contrast Agents: Structure, Dynamics, and Applications. *Chem. Rev.* **1999**, *99*, 2293−2352.
(59) Wang, X. H.; Feng, Y.; Ke, T. Y.; Schabel, M.; Lu, Z. R. Pharmacokinetics and Tissue Retention of (Gd-DTPA)-Cystamine Copolymers, a Biodegradable Macromolecular Magnetic Resonance Imaging Contrast Agent. *Pharm. Res.* **2005**, *22*, 596−602.
(60) Li, T. T.; Qian, Y.; Ye, M. Z.; Tang, J. B.; Hu, H. J.; Shen, Y. Q. Synthesis and Properties of a Biodegradable Dendritic Magnetic Resonance Imaging Contrast Agent. *Chin. J. Chem.* **2014**, *32*, 91−96.

DOI: 10.1021/acsabm.8b00639
ACS Appl. Bio Mater. 2019, 2, 406−416